

# New Description of Molecular Chirality and Its Application to the Prediction of the Preferred Enantiomer in Stereoselective Reactions

João Aires-de-Sousa<sup>†</sup> and Johann Gasteiger<sup>\*,‡</sup>

Secção de Química Orgânica Aplicada, Departamento de Química, Centro de Química Fina e Biotecnologia, campus Faculdade de Ciências e Tecnologia, Universidade Nova de Lisboa, Quinta da Torre, 2825-114 Monte de Caparica, Portugal, and Computer-Chemie-Centrum, Institute for Organic Chemistry, University of Erlangen-Nürnberg, Nögelsbachstrasse 25, D-91052 Erlangen, Germany

Received August 25, 2000

A new representation of molecular chirality as a fixed-length code is introduced. This code describes chiral carbon atoms using atomic properties and geometrical features independent of conformation and is able to distinguish between enantiomers. It was used as input to counterpropagation (CPG) neural networks in two different applications. In the case of a catalytic enantioselective reaction the CPG network established a correlation between the chirality codes of the catalysts and the major enantiomer obtained by the reaction. In the second application—enantioselective reduction of ketones by DIP-chloride—the series of major and minor enantiomers produced from different substrates were clustered by the CPG neural network into separate regions, one characteristic of the minor products and the other characteristic of the major products.

## INTRODUCTION

Molecular chirality is of profound importance in many areas of chemistry. Enantiomers quite often exhibit different chemical and physical properties as well as different biological activity. Thus, the development of enantiomerically pure drugs and agrochemicals has become of great interest. This demands improved enantioselective methods in organic synthesis, in analytical chemistry, and in separation techniques.

Computer-based approaches to property prediction in such areas require an adequate representation of chirality that is able to distinguish between enantiomers. Binary classification as *R* and *S* (or *D* and *L*) is efficient for labeling but not for correlating structures with properties. Three-dimensional atomic coordinates implicitly and accurately represent chirality, but they cannot be used directly as descriptors because of the following reasons: (a) 3D coordinates depend on the position and orientation of the whole molecule in Cartesian space, whereas chirality does not; (b) the number of 3D coordinates depends on the size of a molecule, and, thus, they cannot be used directly to represent a molecule as a fixed-length vector, which is usually required for statistical or computational processing.

On the other hand, representations of the 3D structure on the basis of interatomic distances are not able to differentiate between enantiomers.

Several quantitative measures of chirality have been developed during the past 40 years and were extensively reviewed.<sup>1–3</sup> Mislow et al.<sup>1</sup> distinguished between two classes of measures. In the first “the degree of chirality expresses the extent to which a chiral object differs from an achiral

reference object”. In the second “it expresses the extent to which two enantiomorphs differ from one another”. These methods yield a single real value, usually an absolute quantity that is the same for both enantiomorphs.

Ruch's “chirality functions”<sup>4</sup> are measures of the first kind and can distinguish between enantiomers. Here, a chiral molecule is considered as an achiral “skeleton” with attached “ligands”, each of them characterized by a specific parameter. A polynomial function transforms these parameters into a chirality measure.

Applications of quantitative measures of chirality to the prediction of experimental observables have been quite limited.

Schultz et al.<sup>5</sup> followed a different approach by incorporating *R/S* labels into topological indices, and Julián-Ortiz et al.<sup>6</sup> correlated similar topological indices with pharmacological activity.

Instead of *measuring* chirality by a single value, this paper presents a new molecular transform that *represents* chirality using a fixed set of descriptors. Furthermore, this code includes information about the geometry of chiral centers, properties of the atoms in their neighborhoods, and bond lengths and distinguishes between enantiomers. Additionally, we will show that such a code provides adequate vectors for neural network input. This will be illustrated with the prediction of the major enantiomer in enantioselective reactions.

## METHODOLOGY

**1. Chirality Code.** The outset of our approach was a mathematical transformation of the 3D structure of a molecule into an atomic radial distribution function<sup>7</sup>

$$g(r) = \sum_j \sum_i a_i a_j e^{-b(r-r_{ij})^2} \quad (1)$$

\* To whom correspondence should be addressed. Telephone: 0049-9131-85-6570. Fax: 0049-9131-85-6566. E-mail: gasteiger@chemie.uni-erlangen.de.

<sup>†</sup> Universidade Nova de Lisboa. Telephone: 00351-21-294-8575. Fax: 00351-21-294-8550. E-mail: jas@mail.fct.unl.pt.

<sup>‡</sup> University of Erlangen-Nürnberg.

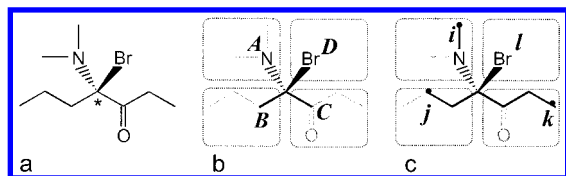


**Figure 1.** (a) Example of a chiral molecule. (b) Atoms A, B, C, and D directly bonded to the chiral center. The neighborhood of atom A is the set of atoms whose distance (in number of bonds) to A is less than their distance to B, C, and D. In cyclic structures different neighborhoods can overlap. (c) Example of a combination of four atoms (*i*, *j*, *k*, and *l*) each at a different ligand (A, B, C, or D) of the chiral center.

In this equation,  $a_i$  and  $a_j$  are properties of atoms *i* and *j* such as atomic number,  $r_{ij}$  is the distance between the atoms *i* and *j*, and  $b$  is a smoothing parameter. The value of  $r$  is a running variable for the function  $g(r)$ .

Such representations of the 3D structure of a molecule are used in X-ray structure powder diffraction experiments. We have recently shown that a molecular encoding scheme can be developed on the basis of eq 1 and have utilized such a representation of the 3D structure of a molecule for the simulation of infrared spectra.<sup>7</sup>

Equation 1 and the encoding of a molecule derived from it cannot, however, distinguish between enantiomers. To take account of the stereochemical situation at a chiral center, first, a value of  $E_{ijkl}$  was defined through eq 2 that considers atoms *i*, *j*, *k*, and *l*, each of them belonging to a different neighborhood of the four atoms A, B, C, and D that are directly bonded to the chiral center (see Figure 1).

$$E_{ijkl} = \frac{a_i a_j}{r_{ij}} + \frac{a_i a_k}{r_{ik}} + \frac{a_i a_l}{r_{il}} + \frac{a_j a_k}{r_{jk}} + \frac{a_j a_l}{r_{jl}} + \frac{a_k a_l}{r_{kl}} \quad (2)$$

$a_i$  is again a property of atom *i*, and  $r_{ij}$  is a distance between atoms *i* and *j*. To consider the 3D structure but make the chirality code independent of a specific conformer,  $r_{ij}$  was taken as the sum of the bond lengths between atoms *i* and *j* on the path with the minimum number of bond counts. Clearly, enantioselectivity is influenced by the conformation of the reacting species, but it is usually an ensemble of conformations that accounts for enantioselectivity. To stay clear of having to decide which conformations determine enantioselectivity, a measure of the 3D structure that is independent of conformational preferences was chosen.

Furthermore, a chirality signal,  $S_{ijkl}$ , was defined that can attain values of +1 or -1. For the computation of  $S_{ijkl}$ , atoms *i*, *j*, *k*, and *l* are ranked according to decreasing atomic property  $a_i$ . When the property of two atoms is the same, the properties of the neighbors (A, B, C, or D) are used for ranking. The 3D coordinates of A are then used for atom *i*, those of B for *j*, those of C for *k*, and those of D for *l*. The first three atoms (in the order established by ranking) define a plane. If they are ordered clockwise and the fourth atom is behind the plane, the chirality signal,  $S_{ijkl}$ , obtains a value of +1. If the geometric arrangement is opposite,  $S_{ijkl}$  obtains a value of -1.

The value of  $E_{ijkl}$  embodies the conformation independent three-dimensional arrangement of the atoms of the ligands of a chirality center in distance space and thus cannot distinguish between enantiomers. This distinction is introduced by the descriptor  $S_{ijkl}$ .

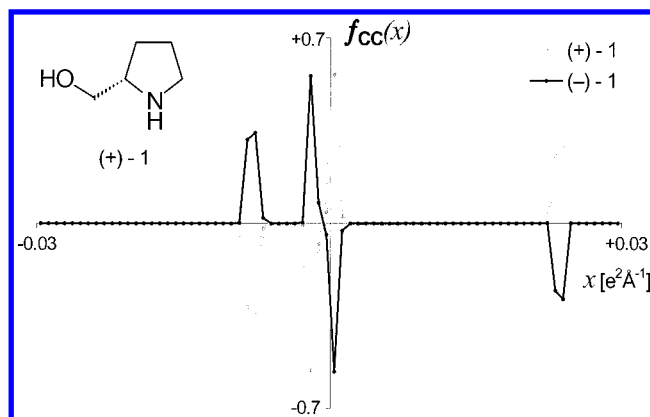


**Figure 2.** Graphical representation of  $f_{cc}(x)$  vs  $x$  for (+)-1 and (-)-1 sampled at 75 evenly distributed points between -0.03 and +0.03  $e^2 \text{ Å}^{-1}$ . Hydrogen atoms not bonded to chiral carbon atoms were not considered.

The two values,  $E$  and  $S$ , calculated for all the combinations of four atoms (each one sampled from a different ligand of a chiral center) are then combined to generate a *chirality code* using

$$f_{cc}(x) = \sum_i \sum_j \sum_k \sum_l S_{ijkl} e^{-B(x-E_{ijkl})^2} \quad (3)$$

$f_{cc}(x)$  is calculated at a number of discrete points with defined intervals to obtain the same number of descriptors, irrespective of the size of the molecule. The actual range of  $x$  used in an application is chosen according to the range of atomic properties related to the range of observed interatomic distances for the given molecules.

The number of discrete points of  $f_{cc}(x)$  determines the resolution of the chirality code.  $B$  is a smoothing factor; in practice  $B$  controls the width of the peaks obtained by a graphical representation of  $f_{cc}(x)$  vs  $x$ . An example of a chirality code for the enantiomers of 1 is shown in Figure 2.

The property,  $a_i$ , of an atom should have values that allow one to distinguish between any nonequivalent atom. For that purpose we have selected the PEOE method<sup>8,9</sup> to calculate partial atomic charges,  $q_i$ , because this method rapidly assigns highly selective values to the atoms of large molecules and sizable datasets.

**2. Counterpropagation Neural Network.** To model the relationship between the chirality code,  $f_{cc}(x)$ , of a given chiral compound and a corresponding chemical property (e.g., enantiomeric preference in an enantioselective reaction) a counterpropagation (CPG) neural network<sup>10</sup> was used. CPG networks were chosen because they are especially useful for the modeling of complex and nonlinear relationships.

The input data for a CPG network are stored in a two-dimensional grid of neurons, each containing as many elements (weights) as there are input variables. In the investigations described in this paper the input variables are discrete points of  $f_{cc}(x)$ , the chirality code. In Figure 3 this part of the CPG network is represented by the upper block, which is basically a Kohonen<sup>11</sup> network. The output data (in this case the chiral property) are stored in a second layer, that acts as a look-up table.

During training of a CPG network, each individual object (chirality code/property pair) is mapped into that neuron of the Kohonen layer (central neuron or winning neuron) that

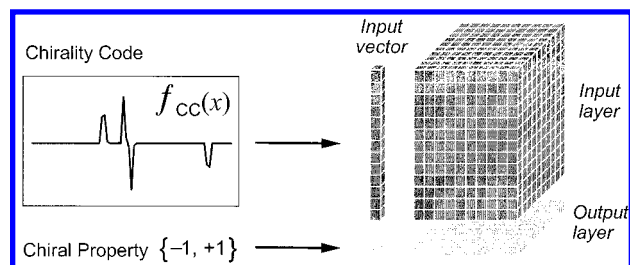


**Figure 3.** Illustration of the CPG neural network method. A chirality code is transformed into a vector with a number of elements equal to the number of weights in the input layer. The CPG neural network stores the chirality codes in the input layer while the corresponding chiral properties are stored in the equivalent positions of the output layer (see text for details).

contains the most similar weights compared to the input data (chirality code). The weights of both input and output layers are then adjusted to make them even more similar to the presented data. The extent of adjustment depends on the topological distance to the central neuron. Note that the property to be investigated, the chiral property, is not used in determining the winning neuron. Thus, it is not of influence on the final mapping; we have an unsupervised learning technique.

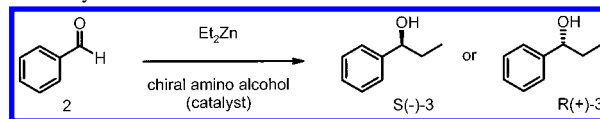
After the training, the CPG network is able to predict a property on input of a chirality code. The winning neuron is chosen, and the correspondent value in the output layer is used for prediction. A trained CPG neural network will reveal similarities in the objects of a dataset in the sense that similar objects (similar chirality codes) are mapped into the same or closely adjacent neurons.

## COMPUTATIONAL DETAILS

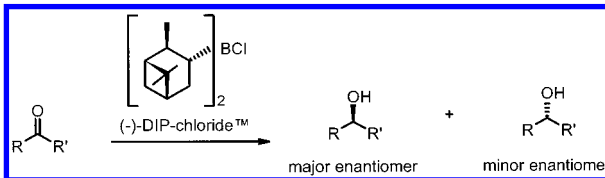
**1. Calculation of Chirality Codes.** The Cartesian coordinates of the atoms in a molecule were calculated from the connection tables of the molecules by the 3D structure generator CORINA.<sup>12–15</sup> The physicochemical atomic properties were calculated using fast empirical methods implemented in the program package PETRA.<sup>8,9</sup> The various physicochemical properties used in the examples are mentioned in the text. The calculation of chirality codes has been performed by a computer program especially developed for this task. The program was written using the C programming language and, for the experiments described here, was compiled for WindowsNT platforms.

**2. Parameters of Counterpropagation Neural Networks.** The CPG networks used in this investigation were simulated with the CPG network simulator KMAP.<sup>16</sup> The networks consist of  $10 \times 10$  or  $15 \times 15$  neurons in a toroidal shape. Each data set used in this investigation has been divided into a training and a test set. The number of data for the individual applications is mentioned in the text. Training of the CPG network was performed by using a linear decreasing triangular scaling function used with an initial learning span of 8 and an initial learning rate of 0.7. The weights were initialized with normally distributed pseudo-random numbers that are calculated using the mean and standard deviation of the input data set as parameters. For the selection of the central neuron the minimum Euclidean distance between the input vector and neuron weights has been used. The training was performed until the learning span was reduced to zero and the learning rate was

**Scheme 1.** Enantioselective Catalytic Addition of Diethylzinc to Benzaldehyde



**Scheme 2.** Enantioselective Reduction of Prochiral Ketones by DIP-chloride



reduced to 0.1, in an unsupervised manner; i.e., the values in the output layer were adapted but not used for the selection of the central neuron.

## RESULTS AND DISCUSSION

In the following applications of the chirality code in the field of enantioselective synthesis two conceptually different situations were investigated in which the chiral source plays a different role in the reaction.

The first study deals with a *catalytic* enantioselective reaction—the enantioselective addition of diethylzinc to benzaldehyde catalyzed by a chiral amino alcohol (Scheme 1).<sup>17,18</sup>

In the second application, the enantioselective reduction of ketones by DIP-chloride has been investigated. This is a representative enantioselective reaction making use of a chiral reagent (Scheme 2).<sup>19</sup>

**1. Prediction of the Major Enantiomer in the Catalytic Addition of Diethylzinc to Benzaldehyde.** The chirality code was computed for a series of 50 amino alcohols (Figure 4) that are known to enantioselectively catalyze the addition of diethylzinc to benzaldehyde. The amino alcohols for this dataset of catalysts were retrieved from the literature,<sup>17,18,20–26</sup> restricted to compounds containing C, N, O, and H atoms only and selected to cover a wide structural diversity.

Each catalyst was described by the chirality code with the partial atomic charges as atomic property at 75 evenly distributed values of  $x$  between  $-0.03$  and  $+0.03$   $e^2 \text{ \AA}^{-1}$  with a smoothing parameter  $B$  of  $6.08 \text{ \AA}^2 e^{-4}$ . Combinations with interatomic distances larger than 10 bonds were excluded, and hydrogen atoms not bonded to chiral carbon atoms were not considered. The resulting 75-dimensional vectors were normalized by their vector sum.

Each input neuron was connected to an output value containing the information about the preferred enantiomer. An output value of  $+1$  was given to the catalysts yielding preferentially  $(+)-3$  and a value of  $-1$  to those yielding preferentially the opposite enantiomer. A CPG network of a dimension of  $10 \times 10$  neurons was trained with 45 catalysts. The trained network was then used to make predictions for a test set of five different catalysts (**48–52**), that were chosen such that several different situations were represented: catalysts with different numbers of chiral carbon atoms; chiral centers directly bonded to N or to O; intuitively different configurations.

Each catalyst of the test set was submitted individually to the trained CPG network; the central neuron was determined,

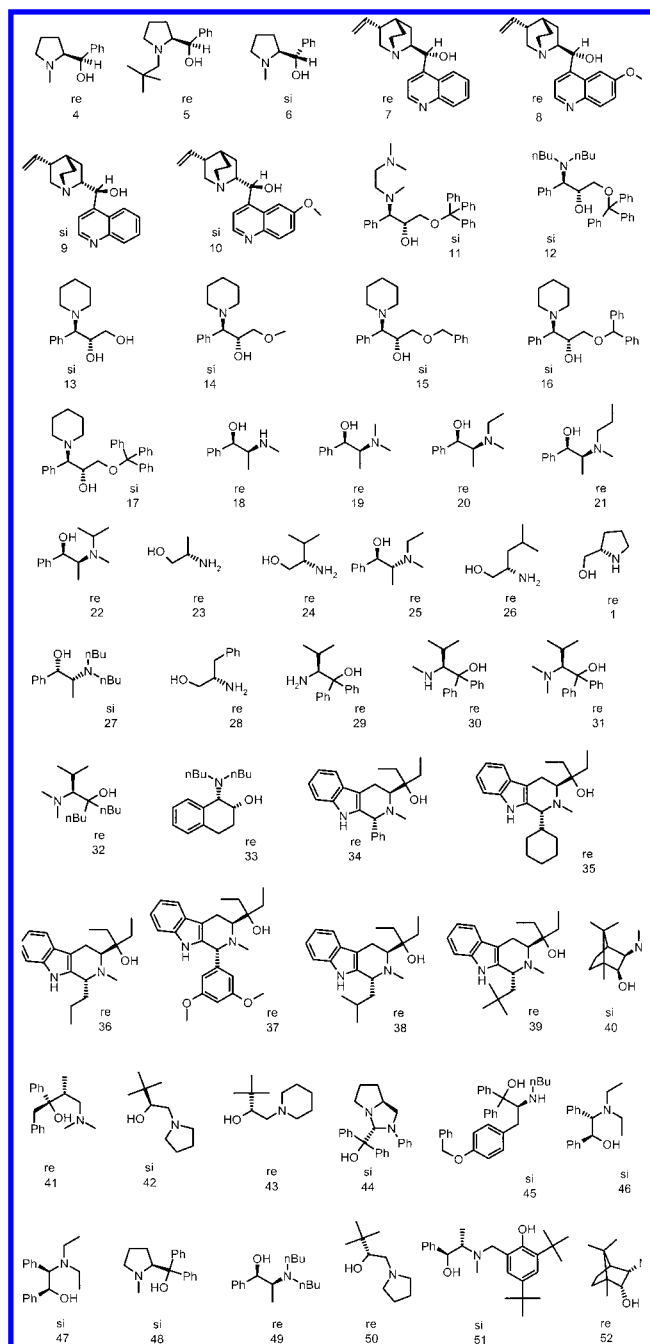


**Figure 4.** Amino alcohols described as catalysts in the addition of diethylzinc to benzaldehyde. Those yielding preferentially (+)-**3** were labeled with "re" and those yielding (–)-**3** were labeled with "si".

and the corresponding neuron in the output layer was selected. The predicted value was based on the weight of the selected output neuron. For the classification of enantiomers a preference for (+)-**3** was predicted if the output value was positive and a preference for (–)-**3** if the output value was negative. The network correctly classified all samples of the test set. The resulting map and the neurons activated by the test set are shown in Figure 5. Note that some neurons have received more than one compound, whereas those shown in white in Figure 5a did not receive any compound at all from the training set.

Despite the large structural diversity of the training set, the catalysts yielding (+)-**3** were clearly mapped into a region different from those that yield the opposite enantiomer. It

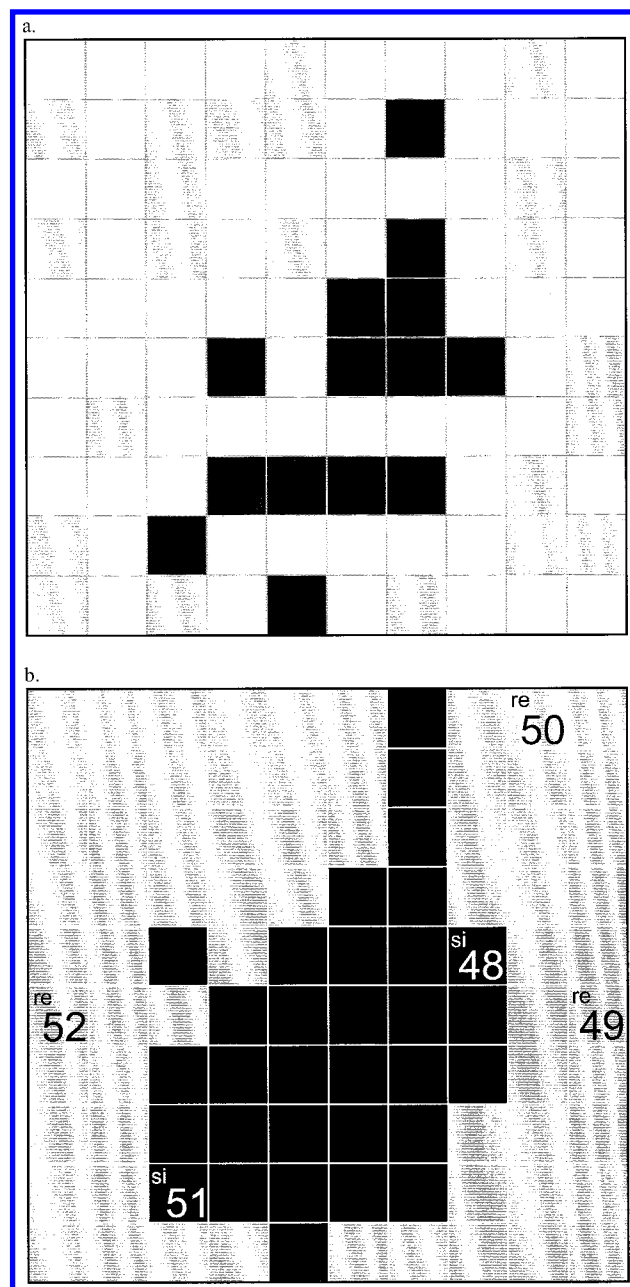


**Figure 5.** (a) Mapping of 45 catalysts into a  $10 \times 10$  CPG network with toroidal surface. Neurons with catalysts yielding preferentially (+)-**3** are displayed in gray; neurons with catalysts yielding preferentially (–)-**3**, in black. (b) Representation of the output weights of the trained CPG network and mapping of the test structures **48–52**. Neurons displayed in gray have a positive output weight, while those displayed in black have a negative output weight. All test examples were correctly classified.

should be emphasized that the training set could well be separated (Figure 5a), although the information of which enantiomer is preferred was not used in determining the winning neuron. All catalysts of the test set were correctly classified.

The mechanism by which the catalyst determines the preference for one enantiomer or the other is influenced by the conformational flexibility of the catalyst and by its complexation with zinc. The characterization of the chiral carbon atoms by the method presented here was able to account for the enantiomeric preference, although those factors were not explicitly included in the chirality code.



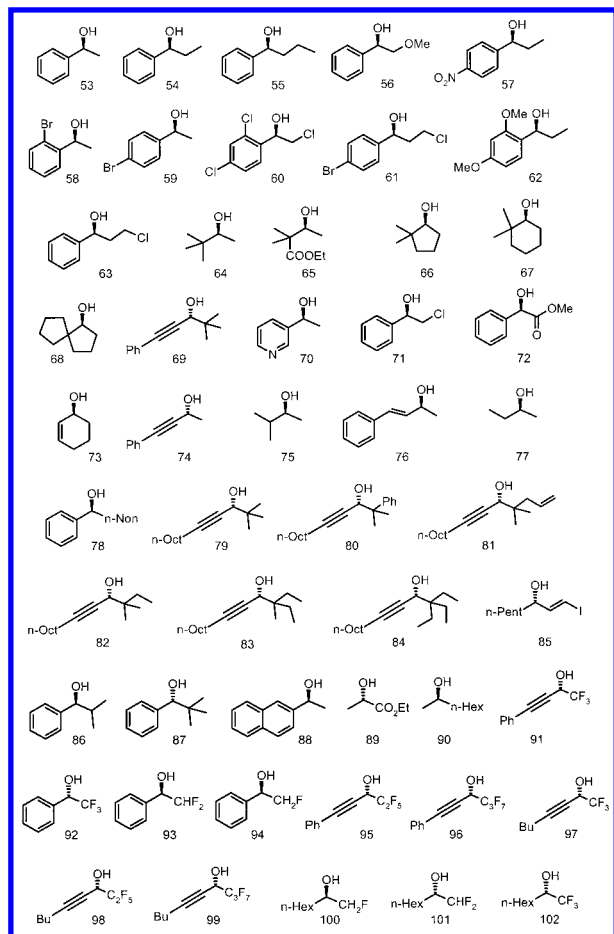


**Figure 6.** Dataset of preferred enantiomers obtained via the reduction of the correspondent ketones by  $(-)$ -DIP-chloride.

This result shows the potential of the new code to store critical information about the chirality of a molecular structure without being affected by the specific conformation adopted.

## 2. Prediction of the Major Enantiomer in Enantioselective Reduction of Ketones by DIP-chloride.

Enantioselective reduction of ketones by DIP-chloride is a well-established synthetic route to chiral alcohols vastly documented in the literature and with a wide scope of application.<sup>19</sup> In this investigation the chirality code was computed for the major and minor enantiomers resulting from the reduction of 50 ketones by  $(-)$ -DIP-chloride (Scheme 2). In selecting this dataset of products (Figure 6) from information in the literature,<sup>19,27–30</sup> care was taken to only consider results from the same laboratory, exclude products with more than one chiral carbon atom, and have a set of products resulting from different classes of ketones (acyclic, cyclic, aralkyl, heterocyclic,  $\alpha$ -halo,  $\alpha$ -keto esters,  $\beta$ -keto esters, acyclic conjugated enones, cyclic conjugated enones, and conjugated ynones).

The possible enantiomers resulting from the reaction were encoded by the chirality code with 31 evenly distributed values of  $x$  between  $-0.03$  and  $+0.03$   $\text{e}^2 \text{\AA}^{-1}$  with smoothing of  $1.0 \text{\AA}^2 \text{e}^{-4}$  and partial atomic charges used as atomic property. Combinations with interatomic distances larger than six bonds were neglected. The resulting 31-dimensional vectors have been normalized by their vector sum.

An output value of  $+1$  was given to the major (or exclusive) enantiomer, and an output of  $-1$  was given to

the minor (or not formed) enantiomer. The relationship between the preference for an enantiomeric route and the chirality code of the possible products was modeled by a CPG network of dimension  $15 \times 15$  and toroidal topology. The network was trained with 45 pairs of enantiomeric alcohols. Ten possible products (**65**, **72**, **87**, **89**, and **91** and their enantiomers) were used for testing. These 10 structures were chosen according to the following criteria: aromatic and nonaromatic substrates; fluorinated and nonfluorinated substrates; three structures were selected intentionally to have a functional group (an ester group) that was not present in the training set.

For classification of the test structures a major product was predicted if the output value was positive and a minor product if the output value was negative. The resulting map and the neurons activated by the test set are shown in Figure 7.

The network correctly classified all samples of the test set except **87**. The reason for the wrong classification of this compound (and its enantiomer) is the inverted configuration of **87** relative to the similar structures **86** or **53**. This is in fact a very particular case that has been explained by Brown<sup>27</sup> as “an artifact of the transition state”. The configurational variability obtained by reduction of fluorinated substrates by  $(-)$ -DIP-chloride remains to a large extent enigmatic.<sup>30</sup> Despite that, the neural network clustered the major enantiomers resulting from these substrates together with the other major products, with the only exception of **93** (mapped between the enantiomers of **97** and **101**).

An interesting result was obtained for test compounds **65**, **72**, and **89**: the trained network was able to accurately predict the configuration of the major enantiomer resulting from the reduction of  $\alpha$ - and  $\beta$ -keto esters although no such case was presented during the training phase. The reason for the correct prediction in situations that have not been explicitly trained is the ability of CPG networks to interpolate in a nonlinear manner within existing data.

Partial atomic charges were chosen as atomic properties as the charge distribution in a molecule is generally one of the most important factors controlling chemical reactions. This fact was confirmed in our investigations: CPG networks more easily recognize the structures yielding a common enantiomeric preference when partial atomic charges were used compared to other atomic properties, e.g., atomic polarizability.

## CONCLUSION

A fixed-length code was introduced to describe the chirality generated by a chiral carbon atom. The applications described in this paper demonstrate the ability of artificial neural networks to correlate the new code with experimental chemical properties of chiral molecules, even if the structural diversity within the dataset is high.

In the catalytic enantioselective addition of diethylzinc to benzaldehyde a counterpropagation neural network discriminated between the chiral catalysts yielding preferentially one enantiomer and those yielding the opposite chiral product.

Using the same methodology based on chirality codes, the major enantiomers obtained in the enantioselective reduction

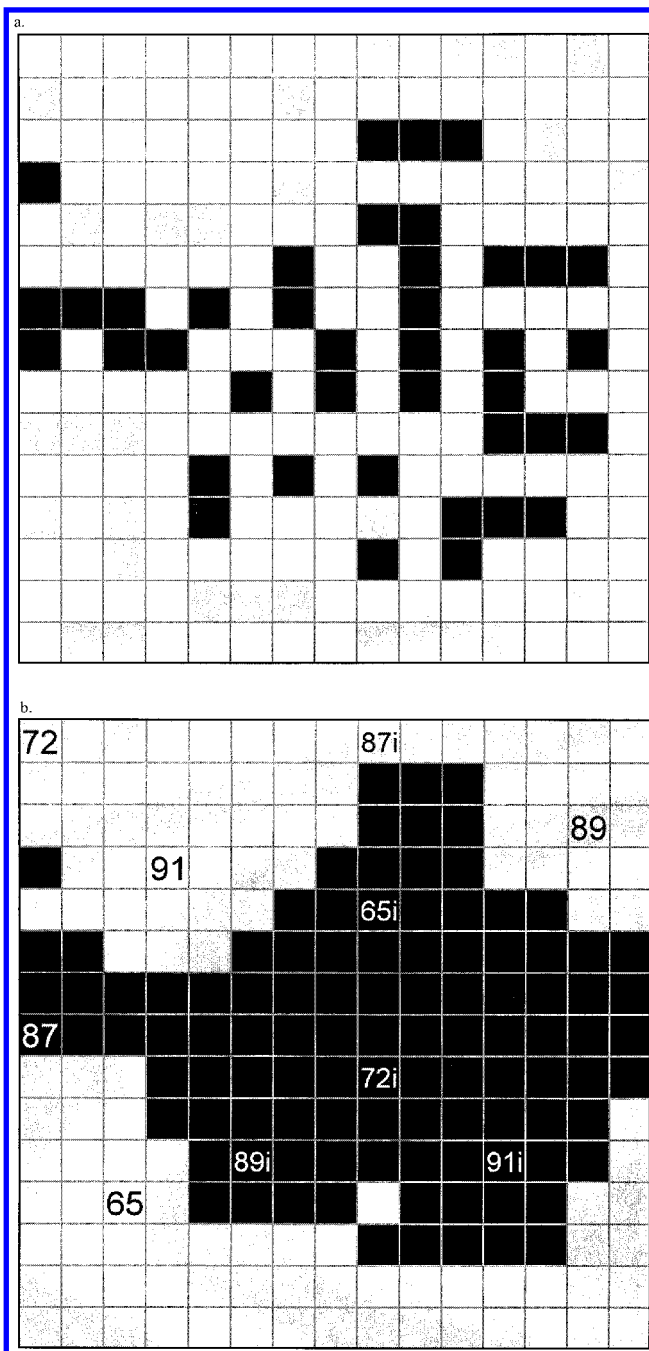


**Figure 7.** (a) Mapping of 90 chiral alcohols into a 15 × 15 CPG network with toroidal surface. Neurons with preferred enantiomers in the reduction by (–)-DIP-chloride are displayed in gray; neurons with minor enantiomers, in black. (b) Representation of the output weights of the trained CPG network and mapping of the test structures **65**, **72**, **87**, **89**, and **91** and the inverted enantiomers (labeled with “i”). Neurons displayed in gray have positive output weights, while those displayed in black have negative output weights.

of ketones with DIP-chloride were discriminated from the minor enantiomers.

Flexibility is one of the most important features of the chirality code. It can be tailored to the desired task by using different atomic properties, by imposing conditions on the atoms that are considered, or by changing functional parameters, like range, resolution, and smoothing.

The method promises to have a wide range of applications, from enantioselective reactions to the study of the biological activity of chiral compounds.

An essential property of the chirality code is that it is independent of conformation. On the other hand, its scope is restricted to central chirality arising from chiral carbon atoms. A complementary approach for a conformation dependent code based on atomic properties and 3D atomic coordinates has also been developed and will be described in a forthcoming publication.

#### ACKNOWLEDGMENT

J.A.S. acknowledges Fundação para a Ciência e a Tecnologia (Lisboa, Portugal) for a postdoctoral fellowship. J.G. thanks the Bundesministerium für Bildung und Forschung (bmb+f; Grant 0311680) and the Fonds der Chemischen Industrie for financial support.

#### REFERENCES AND NOTES

- (1) Buda, A. B.; Heyde, T.; Mislow, K. On Quantifying Chirality. *Angew. Chem., Int. Ed. Engl.* **1992**, *31*, 989–1007; *Angew. Chem.* **1992**, *104*, 1012–1031.
- (2) Avnir, D.; Hel-Or, H. Z.; Mezey, P. G. Symmetry and Chirality: Continuous Measures. In *The Encyclopedia of Computational Chemistry*; Schleyer, P. v. R., Allinger, N. L., Clark, T., Gasteiger, J., Kollman, P. A., Schaefer, H. F., III, Schreiner, P. R., Eds.; John Wiley & Sons: Chichester, U.K., 1998; Vol. 4, pp 2890–2901.
- (3) Zabrodsky, H.; Avnir, D. Continuous Symmetry Measures. 4. Chirality. *J. Am. Chem. Soc.* **1995**, *117*, 462–473.
- (4) Ruch, E. Algebraic Aspects of the Chirality Phenomenon in Chemistry. *Acc. Chem. Res.* **1972**, *5*, 49–56.
- (5) Schultz, H. P.; Schultz, E. B.; Schultz, T. P. Topological Organic Chemistry. 9. Graph Theory and Molecular Topological Indices of Stereoisomeric Organic Compounds. *J. Chem. Inf. Comput. Sci.* **1995**, *35*, 864–870.
- (6) Julián-Ortiz, J. V.; Alapont, C. G.; Ríos-Santamarina, I.; García-Doménech, R.; Gálvez, J. Prediction of Properties of Chiral Compounds by Molecular Topology. *J. Mol. Graphics Modell.* **1998**, *16*, 14–18.
- (7) Hemmer, M. C.; Steinhauer, V.; Gasteiger, J. The Prediction of the 3D Structure of Organic Molecules from Their Infrared Spectra. *Vibrat. Spectrosc.* **1999**, *19*, 151–164.
- (8) Gasteiger, J.; Marsili, M. Iterative Partial Equalization of Orbital Electronegativity—A Rapid Access to Atomic Charges. *Tetrahedron* **1980**, *36*, 3219–3228.
- (9) Gasteiger, J.; Saller, H. Calculation of the Charge Distribution in Conjugated Systems by a Quantification of the Resonance Concept. *Angew. Chem., Int. Ed. Engl.* **1985**, *24*, 687–689; *Angew. Chem.* **1985**, *97*, 699–701.
- (10) For detailed description of neural networks see: (a) Gasteiger, J.; Zupan, J. Neural Networks in Chemistry. *Angew. Chem., Int. Ed. Engl.* **1993**, *32*, 503–527; *Angew. Chem.* **1993**, *105*, 510–536. (b) Zupan, J.; Gasteiger, J. *Neural Networks in Chemistry and Drug Design*, 2nd ed.; Wiley-VCH: Weinheim, Germany, 1999.
- (11) Kohonen, T. *Self-Organization and Associative Memory*, 3rd ed.; Springer: Berlin, 1989.
- (12) Sadowski, J.; Gasteiger, J. From Atoms and Bonds to Three-Dimensional Atomic Coordinates: Automatic Model Builders. *Chem. Rev.* **1993**, *93*, 2567–2581.
- (13) Gasteiger, J.; Rudolph, C.; Sadowski, J. Automatic Generation of 3D-Atomic Coordinates for Organic Molecules. *Tetrahedron Comput. Methodol.* **1992**, *3*, 537–547.
- (14) Sadowski, J.; Rudolph, C.; Gasteiger, J. The Generation of 3D-Models of Host-Guest Complexes. *Anal. Chim. Acta* **1992**, *265*, 233–241.
- (15) Sadowski, J.; Gasteiger, J.; Klebe, G. Comparison of Automatic Three-Dimensional Model Builders Using 639 X-Ray Structures. *J. Chem. Inf. Comput. Sci.* **1994**, *34*, 1000–1008.
- (16) Teckentrup, A. Ph.D. Thesis, University of Erlangen-Nürnberg, Erlangen, Germany, 2000.
- (17) Noyori, R. *Asymmetric Catalysis in Organic Synthesis*; John Wiley & Sons: New York, 1994; pp 255–297.
- (18) Soai, K.; Niwa, S. Enantioselective Addition of Organozinc Reagents to Aldehydes. *Chem. Rev.* **1992**, *92*, 833–856.
- (19) Brown, H. C.; Ramachandran, P. V. Asymmetric Reduction with Chiral Organoboranes Based on  $\alpha$ -Pinene. *Acc. Chem. Res.* **1992**, *25*, 16–24.
- (20) Smaardijk, A. A.; Wynberg, H. Stereoselective Addition Reaction of Diethylzinc to Aldehydes, Catalyzed by Cinchona Alkaloids. *J. Org. Chem.* **1987**, *52*, 135–137.

- (21) Oguni, N.; Omi, T. Enantioselective Addition of Diethylzinc to Benzaldehyde Catalyzed by a Small Amount of Chiral 2-Amino-1-alcohols. *Tetrahedron Lett.* **1984**, 25, 2823–2824.
- (22) Delair, P.; Einhorn, C.; Einhorn, J.; Luche, J. L. New  $\beta$ -Amino Alcohols Derived from L-Valine as Chiral Inductors for Enantioselective Reductions of, and Nucleophilic Additions to Carbonyl Compounds. *Tetrahedron* **1995**, 51, 165–172.
- (23) Vidal-Ferran, A.; Moyano, A.; Pericàs, M. A.; Riera, A. Synthesis of a Family of Fine-Tunable New Chiral Ligands for Catalytic Asymmetric Synthesis. Ligand Optimization through the Enantioselective Addition of Diethylzinc to Aldehydes. *J. Org. Chem.* **1997**, 62, 4970–4982.
- (24) Bellucci, C. M.; Bergamini, A.; Cozzi, P. G.; Papa, A.; Tagliavini, E.; Umani-Ronchi, A. Catalytic Asymmetric Synthesis of Secondary Alcohols Using Chiral *cis*-1-Amino-2-hydroxy-1,2,3,4-tetrahydronaphthalene as Chiral Ligand. *Tetrahedron: Asymmetry* **1997**, 8, 895–902.
- (25) Dai, W.-M.; Zhu, H. J.; Hao, X.-J. Chiral Ligands Derived from *Abrine*. 3. Asymmetric Pictet–Spengler Reaction of *Abrine* Methyl Ester and Synthesis of Chiral 1,2,3,4-Tetrahydro- $\beta$ -carbolines as Promoters in Addition of Diethylzinc toward Aromatic Aldehydes. *Tetrahedron Lett.* **1996**, 37, 5971–5974.
- (26) Chaloner, P. A.; Perera, S. A. R. Enantioselective Addition of Diethylzinc to Benzaldehyde in the Presence of Ephedrine Derivatives. *Tetrahedron Lett.* **1987**, 28, 3013–3014.
- (27) Brown, H. C.; Chandrasekharan, J.; Ramachandran, P. V. Chiral Synthesis via Organoboranes. 14. Selective Reductions. 41. Diisopinocampheylchloroborane, an Exceptionally Efficient Chiral Reducing Agent. *J. Am. Chem. Soc.* **1988**, 110, 1539–1546.
- (28) Ramachandran, P. V.; Teodorovici, A. V.; Rangaishenvi, M. V.; Brown, H. C. Chiral Synthesis via Organoboranes. 34. Selective Reductions. 47. Asymmetric Reductions of Hindered  $\alpha,\beta$ -Acetylenic Ketones with *B*-Chlorodiisopinocampheylborane to Propargylic Alcohols of Very High Enantiomeric Excess. Improved Workup Procedure for the Isolation of Product Alcohols. *J. Org. Chem.* **1992**, 57, 2379–2386.
- (29) Ramachandran, P. V.; Gong, B.; Teodorovici, A. V.; Brown, H. C. Selective Reductions. 52. Efficient Asymmetric Reduction of  $\alpha$ -Acetylenic  $\alpha'$ -Fluoroalkyl Ketones with Either *B*-Chlorodiisopinocampheylborane or *B*-Isopinocampheyl-9-borabicyclo[3.3.1]nonane in High Enantiomeric Purity. The Influence of Fluoro Groups in Such Reductions. *Tetrahedron: Asymmetry* **1994**, 5, 1061–1074.
- (30) Ramachandran, P. V.; Teodorovici, A. V.; Gong, B.; Brown, H. C. Selective Reductions. 53. Asymmetric Reduction of  $\alpha$ -Fluoromethyl Ketones with *B*-Chlorodiisopinocampheylborane and *B*-Isopinocampheyl-9-borabicyclo[3.3.1]nonane. Combined Electronic and Steric Contributions to the Enantiocontrol Process. *Tetrahedron: Asymmetry* **1994**, 5, 1075–1086.

CI000125N